Video Article

Preparation and Use of Photocatalytically Active Segmented Ag|ZnO and Coaxial TiO_2-Ag Nanowires Made by Templated Electrodeposition

A. Wouter Maijenburg[1], Eddy J.B. Rodijk[1], Michiel G. Maas[1], Johan E. ten Elshof[1]

[1]MESA+ Institute for Nanotechnology, University of Twente

Correspondence to: Johan E. ten Elshof at j.e.tenelshof@utwente.nl

URL: https://www.jove.com/video/51547
DOI: doi:10.3791/51547

Keywords: Physics, Issue 87, Multicomponent nanowires, electrochemistry, sol-gel processes, photocatalysis, photochemistry, H_2 evolution

Date Published: 5/2/2014

Citation: Maijenburg, A.W., Rodijk, E.J., Maas, M.G., ten Elshof, J.E. Preparation and Use of Photocatalytically Active Segmented Ag|ZnO and Coaxial TiO_2-Ag Nanowires Made by Templated Electrodeposition. *J. Vis. Exp.* (87), e51547, doi:10.3791/51547 (2014).

Abstract

Photocatalytically active nanostructures require a large specific surface area with the presence of many catalytically active sites for the oxidation and reduction half reactions, and fast electron (hole) diffusion and charge separation. Nanowires present suitable architectures to meet these requirements. Axially segmented Ag|ZnO and radially segmented (coaxial) TiO_2-Ag nanowires with a diameter of 200 nm and a length of 6-20 µm were made by templated electrodeposition within the pores of polycarbonate track-etched (PCTE) or anodized aluminum oxide (AAO) membranes, respectively. In the photocatalytic experiments, the ZnO and TiO_2 phases acted as photoanodes, and Ag as cathode. No external circuit is needed to connect both electrodes, which is a key advantage over conventional photo-electrochemical cells. For making segmented Ag|ZnO nanowires, the Ag salt electrolyte was replaced after formation of the Ag segment to form a ZnO segment attached to the Ag segment. For making coaxial TiO_2-Ag nanowires, a TiO_2 gel was first formed by the electrochemically induced sol-gel method. Drying and thermal annealing of the as-formed TiO_2 gel resulted in the formation of crystalline TiO_2 nanotubes. A subsequent Ag electrodeposition step inside the TiO_2 nanotubes resulted in formation of coaxial TiO_2-Ag nanowires. Due to the combination of an *n*-type semiconductor (ZnO or TiO_2) and a metal (Ag) within the same nanowire, a Schottky barrier was created at the interface between the phases. To demonstrate the photocatalytic activity of these nanowires, the Ag|ZnO nanowires were used in a photocatalytic experiment in which H_2 gas was detected upon UV illumination of the nanowires dispersed in a methanol/water mixture. After 17 min of illumination, approximately 0.2 vol% H_2 gas was detected from a suspension of ~0.1 g of Ag|ZnO nanowires in a 50 ml 80 vol% aqueous methanol solution.

Video Link

The video component of this article can be found at https://www.jove.com/video/51547/

Introduction

Owing to their small dimensions and large surface-to-volume ratio, nanowires are very promising one-dimensional objects that can be used in a wide range of biomedical and nanotechnological applications[1]. In the literature, many nanowires containing a single component with functional properties have been reported[2-7]. But when multiple materials (metals, polymers and metal oxides) are incorporated sequentially within a single nanowire, multifunctional nanowires can be made[8,9]. When several segments are connected inside a single nanowire, functional properties may appear that were not present when only the individual segments were used. For instance, nanomotors containing Au and Pt segments within a single nanowire were reported that moved autonomously when placed in hydrogen peroxide[4]. Suitable techniques for the formation of multisegmented nanowires are infiltration and templated electrodeposition[8,9].

In 1987, Penner and Martin were the first to publish the use of templated electrodeposition for the formation of Au nanowires in polycarbonate membranes[10]. Since then, many other researchers have started using templated electrodeposition for the synthesis of nanowires with different dimensions, using either polycarbonate track-etched membranes (PCTE) or anodized aluminum oxide (AAO) membranes and templates[11]. The advantages of using templated electrodeposition for nanowire synthesis are its cost-effective nature as electrodeposition is usually performed under mild conditions, the possibility to form nanowires from either metals, metal oxides and/or polymers, and its ability to create an exact negative replica of the template used[11]. Furthermore, segmented nanowires can be formed by sequential deposition of two or more different phases, and when a nanotube of one of the two phases can be made by templated electrodeposition, coaxial nanowires containing two different phases can be made.

Metal oxides can be electrodeposited when the respective metal ions are insoluble in aqueous solutions at high pH. For the necessary oxygen, three different precursors can be used, *i.e.* nitrate ions[12-15], hydrogen peroxide[13,16,17], and molecular oxygen[18]. With the use of nitrate ions, as in this protocol, application of a potential more negative than -0.9 V vs. Ag/AgCl leads to a locally increased pH by reduction of nitrate at the cathode[19,20]:

$$NO_3^- + H_2O + 2e^- \rightarrow NO_2^- + 2OH^-. \quad (1)$$

When the electrolyte solution is heated to 60-90 °C, ZnO nanowires will form from precipitated zinc hydroxide:

$Zn^{2+} + 2OH^- \rightarrow ZnO + H_2O$. (**2**)

Upon application of a potential to the working electrode, which is positioned at the pore bottom in templated electrodeposition, the pH inside the pore is locally increased resulting in local nanowire formation. Since ZnO is an *n*-type semiconductor, reactions (1) and (2) can continue at the ZnO/electrolyte interface, resulting in the formation of a crystalline and dense ZnO nanowire[21,22].

Several methods exist for the synthesis of TiO_2 nanotubes, but for the formation of a coaxial structure using a sequential electrodeposition process, the electrochemically induced sol-gel method is most suitable. This method for cathodic electrodeposition of TiO_2 films was first introduced by Natarajan *et al.* in 1996 [23]. and was further improved by Karuppuchamy *et al.* in 2001 [19,24]. Using this method, titanium oxysulfate ($TiOSO_4$) powder is dissolved in an aqueous solution of hydrogen peroxide (H_2O_2) upon the formation of a peroxotitanate complex ($Ti(O_2)SO_4$):

$TiOSO_4 + H_2O_2 \rightarrow Ti(O_2)SO_4 + H_2O$. (**3**)

At potentials more negative than -0.9 V vs. Ag/AgCl, the pH at the electrode surface is increased by reduction of nitrate (reaction (1)), forming a titanium hydroxide gel[19,20]:

$Ti(O_2)SO_4 + 2OH^- + (x+1)\ H_2O \rightarrow TiO(OH)_2.xH_2O + H_2O_2 + SO_4^{2-}$. (**4**)

Natarajan *et al.* used differential thermal analysis to find that water is removed from the gel around 283 °C during thermal annealing, which results in the formation of an amorphous TiO_2 phase[23]. For a planar film, crystallization into the anatase phase occurs when the temperature is increased above 365 °C[23,25], while crystallization occurs at a temperature between 525 and 550 °C when an AAO template is used[25].

$TiO(OH)_2 \cdot xH_2O \rightarrow TiO_2 + (x+1)H_2O$. (**5**)

The pore diameter of the AAO template used determines whether a solid nanowire or open nanotube will be formed. Deposition in a template with a small pore diameter (~50 nm) results in nanowire formation[20,26], while applying the same method inside a pore with larger diameter (~200 nm) results in nanotube formation[25]. This is because gel collapse can take place upon removal of excess water.

In the early 1970s, Fujishima and Honda were the first to publish a system for direct water splitting under UV light, which was accomplished by a rutile electrode coupled to a platinum electrode[27,28]. Since then, over 130 semiconductor materials were identified as photocatalysts[29-31]. Of these, titanium dioxide[32-36], zinc oxide[37-40], and iron oxide[41,42] are among the most intensively studied materials. The surface-to-volume ratio of these materials can be increased drastically when nanoparticles or nanowires are used, leading to improved photocatalytic efficiencies[29,30,43-49].

For the construction of photocatalytic Ag|ZnO nanowires, ZnO, which is a photoactive *n*-type semiconductor, was connected with Ag via sequential electrodeposition inside the same template[50]. Within such a single nanowire, the ZnO photoanode and Ag cathode are directly coupled without the need of an external circuit connecting the electrodes, which is in contrast to the situation in conventional photo-electrochemical cells. This simplifies device architecture considerably and increases the efficiency by reduction of Ohmic losses in the system. ZnO and Ag segments were coupled since the electron affinity of ZnO (4.35 eV vs. vacuum) is very close to the work function of Ag (4.26 eV vs. vacuum). This induces the formation of a Schottky barrier between both phases[51], which allows excited electrons in the conduction band of ZnO to flow to Ag, but not vice versa, thus prohibiting the chance of electron-hole recombination[52]. The active wurtzite phase of ZnO can be formed already at 60-90 °C, which provides an easy and cost effective way of nanowire formation. This is in contrast to most other photoactive oxides that require an intermediate annealing step at high temperatures when made via cathodic electrodeposition.

The conversion of methanol and water into hydrogen and carbon dioxide was used as a model reaction to demonstrate the use of a segmented nanowire containing a metal and a metal oxide phase for autonomous H_2 formation under the influence of UV light. In this experiment, methanol is used as a hole scavenger which is oxidized to CO_2 at the ZnO segment, following the net reaction

$CH_3OH + H_2O + 6h^+ \rightarrow CO_2 + 6H^+$, (**6**)

where h^+ represents an electron hole. The protons formed at the ZnO segment are reduced to H_2 at the Ag surface, following the reaction

$2H^+ + 2e^- \rightarrow H_2$. (**7**)

Since the total energy required for reactions (6) and (7) is much smaller than the band gap of ZnO (0.7 and 3.2 eV, respectively), this process can take place without the need for an external power source. This process is schematically illustrated in **Figure 1**.

In this protocol, the experimental procedures of templated electrodeposition for the formation of segmented and coaxial nanowires containing both a metal and a semiconductor phase are explained. A procedure for the formation of segmented Ag|ZnO nanowires is outlined, as well as the formation of TiO_2 nanotubes and their subsequent filling with Ag to yield coaxial TiO_2-Ag nanowires. Furthermore, the photocatalytic activity of the Ag|ZnO nanowires is demonstrated by converting a methanol/water mixture into H_2 and CO_2 gas upon irradiation with UV light employing a Pd-based sensor for H_2 detection. The emphasis of this protocol is on the preparation and photocatalytic characterization of two differently segmented metal oxide|metal nanowire modules, and a more in-depth treatment and an example of a multifunctional nanowire can be found elsewhere[53]. The water splitting reaction that was employed using the coaxial TiO_2-Ag nanowires can also be found elsewhere[25].

Protocol

Segmented Ag|ZnO Nanowire Formation in PCTE Membranes

1. PCTE Membrane Preparation for Templated Electrodeposition

1. Choose a track-etched polycarbonate membrane with an outer pore diameter of 200 nm and a thickness of 6 µm (**Figure 2a**). The diameter of the membrane used here is 25 mm.
2. Sputter a gold layer at the backside of the membrane (**Figure 2b**). In this case, a deposition pressure of 2 x 10^{-2} mbar was used with Ar as sputtering gas. Use a slow deposition rate of ~13 nm/min. NOTE: This Au layer will be used as electrical contact during electrodeposition.
3. Use double-sided sticky tape to attach a small glass slide (1.4 x 2.1 cm) on top of the gold-coated side of the membrane. For this, put four small strips of double-sided tape along the edges of the glass slide (**Figure 2c**). NOTE: Make sure the membrane is as smooth as possible, without any folds or wrinkles. This glass slide is used to ensure selective electrodeposition inside the membrane pores.
4. Stick a small piece of copper tape on the part of the membrane that sticks out from the glass slide for mechanical stability. Since copper tape is conducting, the crocodile clip of the working electrode can be attached to the copper tape.
5. If necessary, improve the adhesion of the membrane to the glass slide by putting Teflon tape around the edges. NOTE: For depositions at room temperature the adhesion of double-sided tape is usually strong enough, but at elevated temperatures it is recommended to use Teflon tape as well.

2. Electrodeposition of Ag|ZnO Nanowires

1. Preparation of the Ag segment
    1. Prepare an aqueous solution containing 0.20 M $AgNO_3$ (1.70 g per 50 ml) and 0.10 M H_3BO_3 (0.31 g per 50 ml). Adjust the pH to 1.5 using HNO_3.
    2. Put the prepared membrane together with a Pt counter electrode and an Ag/AgCl (3 M KCl) reference electrode in the as-prepared solution.
    3. Apply a potential of +0.10 V vs. the Ag/AgCl reference electrode for 30 sec (**Figures 2d** and **2e**). NOTE: Although every potentiostat software will be different, all programs should have input lines like "set potential" and "duration", where these values can be filled in. Please refer to the potentiostat manual and included software for more details.
    4. Take the electrodes from the solution and rinse them with milli-Q water.

2. Preparation of the ZnO segment
    1. Prepare an aqueous solution containing 0.10 M $Zn(NO_3)_2{\cdot}6H_2O$ (1.49 g per 50 ml).
    2. Heat the solution to 60 °C using a water bath, and put the membrane containing the Ag segment together with a Pt counter electrode and an Ag/AgCl reference electrode in the heated solution.
    3. Apply a potential of -1.00 V vs. the Ag/AgCl reference electrode for 20 min (**Figures 2d** and **2e**). NOTE: Although every potentiostat program will be different, all should have input lines like "set potential" and "duration", where these values can be filled in. Please refer to the potentiostat manual and included software for more details.
    4. Take the electrodes from the solution and rinse them with milli-Q water.

3. Repeat this procedure 4x to obtain enough nanowires for significant signal from the H_2 sensor.

3. Extraction of the Nanowires and Transfer to Aqueous Solution

1. Cut the membrane containing the nanowires from the glass slide.
2. Transfer this part of the membrane to a polypropylene centrifuge tube.
3. Add ~2 ml of CH_2Cl_2 to dissolve the PCTE membrane and release the nanowires into the solution. After ~30 min, the membrane should be completely dissolved (**Figures 2f** and **2g**).
4. Apply a small droplet of the CH_2Cl_2 solution containing nanowires on a small Si wafer for SEM analysis.
5. Centrifuge the obtained solution at ~19,000 x g for 5 min, remove the excess CH_2Cl_2, and add fresh CH_2Cl_2. Repeat the process at least 3x to make sure all polycarbonate has been removed.
6. After all polycarbonate has been removed, add milli-Q water to the nanowires after removal of the excess CH_2Cl_2. Repeat the centrifugation at least 3x again to completely replace all CH_2Cl_2 by milli-Q water.

Coaxial TiO_2-Ag Nanowire Formation in AAO Membranes

4. AAO Membrane Preparation for Templated Electrodeposition

1. Take an AAO membrane with a pore size of 200 nm and thickness of 60 µm (**Figure 2a**). The diameter of the membrane used here is 13 mm.
2. Sputter a gold layer on the backside of the membrane (**Figure 2b**). In this case a deposition pressure of 2 x 10^{-2} mbar was used with Ar as sputtering gas. Use a slow deposition rate of ~13 nm/min. NOTE: This Au layer will be used as electrical contact during electrodeposition.
3. Attach the AAO membranes to an Au-coated glass slide in a configuration as in **Figure 2h** using Teflon tape. NOTE: To ensure selective electrodeposition inside the membrane pores, the AAO membrane needs to be attached to a small glass slide in a different configuration than

the PCTE membranes, because the AAO membranes are too brittle for connection with a crocodile clip. When a glass slide of 3.0 x 2.5 cm is used, two membranes can be used at once.

4. Put a small piece of copper tape on the Au coated part of the glass slide for easy handling when connecting the electrodes.

5. Electrochemical Deposition of TiO_2-Ag Nanowires

1. Preparation of a TiO_2 gel
    1. Prepare an aqueous solution containing 0.02 M $TiOSO_4$ (0.16 g per 50 ml), 0.03 M H_2O_2 (0.13 ml per 50 ml), 0.05 M HNO_3 (0.15 ml per 50 ml), and 0.25 M KNO_3 (1.26 g per 50 ml).
    2. Put the prepared membrane together with a Pt counter electrode and an Ag/AgCl (3 M KCl) reference electrode in the as-prepared solution.
    3. Apply a potential of -1.0 V vs. the Ag/AgCl reference electrode for 3.5 hr (**Figures 2d** and **2e**). NOTE: Although every potentiostat software will be different, all programs should have input lines like "set potential" and "duration", where these values can be filled in. Please refer to the potentiostat manual and included software for more details.
    4. Take the electrodes from the solution and DO NOT rinse the membrane with milli-Q water, because the TiO_2 gel is still water soluble. The other electrodes can be rinsed with milli-Q water.

2. Preparation of coaxial TiO_2-Ag nanowires
    1. Thermally anneal the membranes with the TiO_2 gel in an oven at 650 °C for 2 hr in air.
    2. Reattach the membranes to a gold coated glass slide.
    3. Prepare an aqueous solution containing 0.20 M $AgNO_3$ (1.70 g per 50 ml) and 0.10 M H_3BO_3 (0.31 g per 50 ml). Adjust the pH to 1.5 using HNO_3.
    4. Put the prepared membrane together with a Pt counter electrode and an Ag/AgCl (3 M KCl) reference electrode in the as-prepared solution.
    5. Apply a potential of +0.10 V vs. the Ag/AgCl reference electrode for 1.5 min (**Figures 2d** and **2e**). NOTE: Although every potentiostat software will be different, all programs should have input lines like "set potential" and "duration", where these values can be filled in. Please refer to the potentiostat manual and included software for more details.
    6. Take the electrodes from the solution and rinse them with milli-Q water.

3. Preparation of Ag nanoparticles incorporated in TiO_2 nanotubes
    1. Heat the membranes with the TiO_2 gel overnight at 100 °C.
    2. Prepare an aqueous solution containing 0.20 M $AgNO_3$ (1.70 g per 50 ml) and 0.10 M H_3BO_3 (0.31 g per 50 ml). Adjust the pH to 1.5 using HNO_3.
    3. Put the prepared membrane together with a Pt counter electrode and an Ag/AgCl (3 M KCl) reference electrode in the as-prepared solution.
    4. Apply a potential of +0.10 V vs. the Ag/AgCl reference electrode for 1.5 min (**Figures 2d** and **2e**). NOTE: Although every potentiostat software will be different, all programs should have input lines like "set potential" and "duration", where these values can be filled in. Please refer to the potentiostat manual and included software for more details.
    5. Take the electrodes from the solution and rinse them with milli-Q water.

4. Repeat this procedure to obtain at least 10 membranes filled with nanowires/nanotubes to obtain enough material for significant signal from the H_2 sensor.

6. Extraction of Nanotubes and Nanowires

1. Cut the membrane containing the nanotubes or nanowires from the glass slide.
2. Transfer this part of the membrane into a polypropylene centrifuge tube.
3. Add ~2 ml of an aqueous solution containing 1.0 M NaOH to dissolve the AAO membrane and release the nanotubes or nanowires into the solution. After ~2 hr, the membrane should be completely dissolved (**Figures 2f** and **2g**).
4. Centrifuge the obtained solution at ~19,000 x g for 5 min, remove the excessive NaOH solution, and add fresh milli-Q water. Repeat the process at least 3x to make sure all NaOH has been removed.
5. After all NaOH has been removed, the aqueous suspension can be used for H_2 formation experiments.
6. Alternatively, add CH_2Cl_2 or another volatile solvent to the nanotubes and nanowires after removal of excess water for visualization of the prepared nanotubes or nanowires with SEM. Repeat the centrifugation at least 3x to completely replace all water by the volatile solvent. Deposit a small droplet of the solution containing nanotubes or nanowires onto a small Si wafer.

H_2 Formation Experiments

7. Preparation of the Hydrogen Sensor

1. Take a Pd-based hydrogen sensor.
2. Place the sensor inside an NS plug that fits on top of a quartz tube.
3. Connect the sensor to a standard Wheatstone bridge as illustrated in **Figure 3**.

8. Photocatalytic Hydrogen Formation

1. Put the aqueous nanowire solution in a 72 ml quartz tube. Add more water until a total of 10 ml water is inside the quartz tube. Then add 40 ml methanol.
2. Start recording the signal from the Pd based H_2 sensor before placing it on top of the quartz tube and monitor the variation in signal.
3. After ~200 sec of stable signal, put the H_2 sensor on top of the quartz tube while simultaneously turning on the UV light source to start the actual measurement. NOTE: In these experiments, the UV source was placed approximately 10-15 cm away from the sample.

Representative Results

During electrodeposition, the current that is measured between the working and counter electrodes can be visualized in an I-t curve. Since the current is directly related to the amount of deposited material via Faraday's law, the observed current is an important indication of how the deposition proceeds. Typical I-t curves for the deposition of Ag|ZnO and TiO_2-Ag nanowires are shown in **Figure 4**. Typical SEM images of Ag|ZnO nanowires, TiO_2 nanotubes, a coaxial TiO_2-Ag nanowire and TiO_2/Ag nanotubes can be found in **Figure 5** and **Figure 6**, respectively.

Using the electrochemically induced sol-gel method for deposition of a titania gel inside the template and sequential electrodeposition of Ag can result in two different structures depending on the temperature used to dry the gel. Drying of the gel overnight at 100 °C results in condensation of the gel, preventing it to redissolve in water. Since no dense tubular shape has yet formed at this temperature, Ag nuclei are deposited inside the titania gel. Subsequent annealing at 650 °C results in the formation of Ag nanoparticles incorporated in a TiO_2 nanotube (**Figure 6c**), since the collapse of the titania gel causes the Ag nanoparticles to be transported to the pore walls. In contrast, high temperature annealing of the titania gel prior to Ag electrodeposition leads to the formation of solid TiO_2 nanotubes. In this case, Ag nanowires could be deposited inside these tubes, leading to the formation of TiO_2-Ag nanowires with a coaxial architecture (**Figure 6b**).

The activity of the segmented Ag|ZnO nanowires in photocatalytic water splitting can be investigated using a methanol/water solution under UV illumination, where methanol acts as a hole scavenger. A technically simple method to detect gaseous hydrogen evolving from the solution is obtained by placing a H_2 sensor directly above the solution (**Figure 7**). This experiment only detects the amount of H_2 reaching the sensor, so the actual amount of formed H_2 may be higher as some H_2 will remain dissolved in the methanol/water phase. The signal as detected by the sensor is shown in **Figure 8a**. **Figure 8b** shows the same signal after transformation to the timeframe of actual H_2 formation. When the UV light source was turned on (t = 17.5 min in **Figure 8a**), the signal drops substantially due to the light sensitivity of the sensor. Right after this drop in signal, the reaction starts and consequently this moment was defined as t = 0 min in **Figure 8b**, and the corresponding signal was defined as 0 V. During UV exposure of the test tube, it was also visible that small gas bubbles were formed. Since the sensor used is slightly cross-sensitive to methanol, the measurement of a reference sample without nanowires was also included. During UV illumination, **Figure 8** shows that the signal from the sample with nanowires is higher than the signal from the reference sample.

The increase in potential is a relative measure for the amount of gaseous H_2 that forms and evolves from the solution. In order to give a quantitative estimate for the amount of evolved H_2, the potential response of the sensor from the photocatalytic experiments was compared with its response in a 4 vol% H_2 in N_2 gas stream. From the comparison, it was estimated that 17 min of UV illumination of the Ag|ZnO nanowires resulted in the formation of approximately 0.2 vol% H_2 in the gas volume above the solution. Since ~0.1 g of nanowires was used, this equals to a H_2 evolution rate of 6.92 x 10^{-6} mol/hr·g. As reference, experiments with single-phase ZnO or Ag nanowires were also performed. These experiments, not shown here, did not give any indication of H_2 formation; neither from gas bubble formation nor from sensor signal.

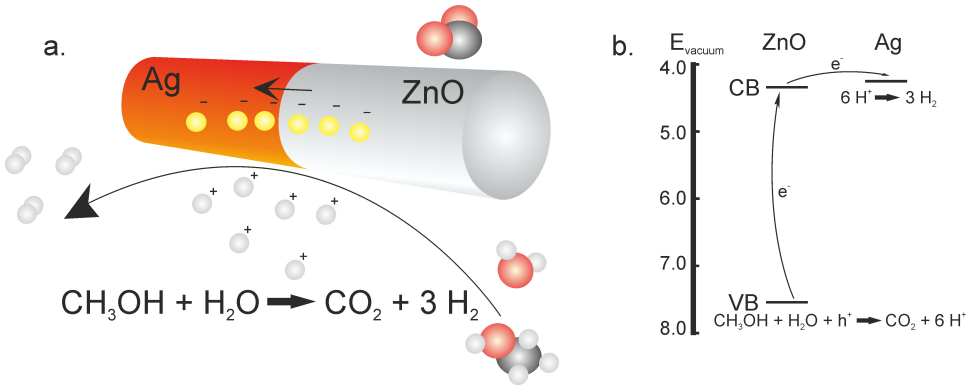

Figure 1. Working principle of segmented Ag|ZnO nanowire in photocatalytic water splitting: (**a**) schematic representation, and (**b**) energy diagram. When UV light is absorbed by the ZnO segment, an electron-hole pair is formed. The as-formed electrons flow to the Ag phase where they are consumed in an electrochemical reduction half-reaction. The hole stays in the ZnO segment where it is consumed in an oxidative half-reaction. Click here to view larger image.

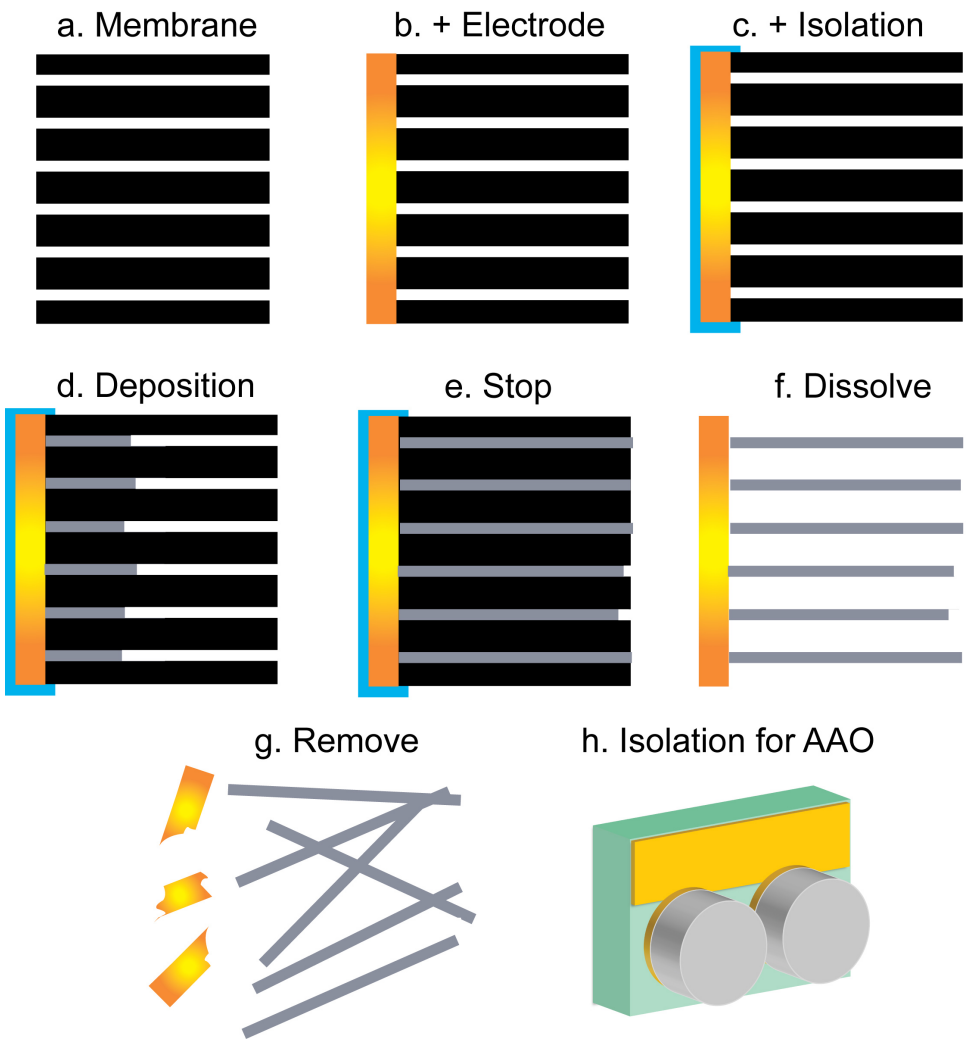

Figure 2. Schematic representation of the consecutive steps taken for nanowire synthesis.

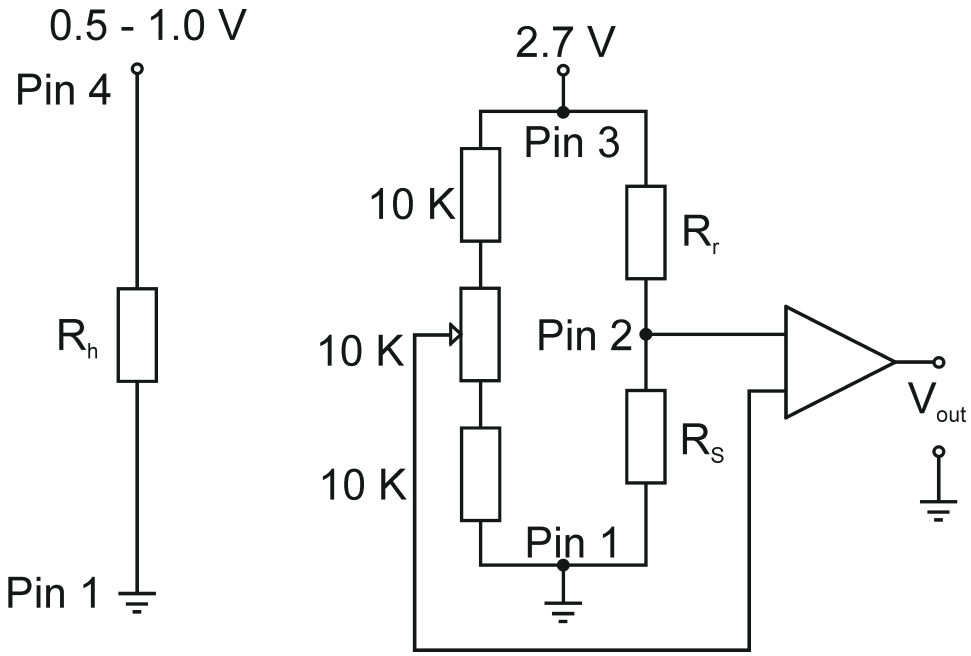

Figure 3. Typical operating circuit of the H_2 sensor with Wheatstone bridge. In this scheme, pin 1 to 4 refer to the wiring of the sensor (pin 1 is black, pin 2 is blue, pin 3 is white, pin 4 is brown), R_h is the resistance of the heater (150 ± 50 Ω), R_r is the resistance of the reference (1,500 ± 500 Ω), R_s is the resistance of the sensor (1,000 ± 250 Ω). The sensor is connected to a 12 V power source so that 0.5 to 1.0 V is applied to the heater and 2.7 V is applied to the Wheatstone bridge. V_{out} is connected to the multimeter/potentiostat. The resistance next to pin 2 is variable and can be adjusted in order to obtain an appropriate baseline.

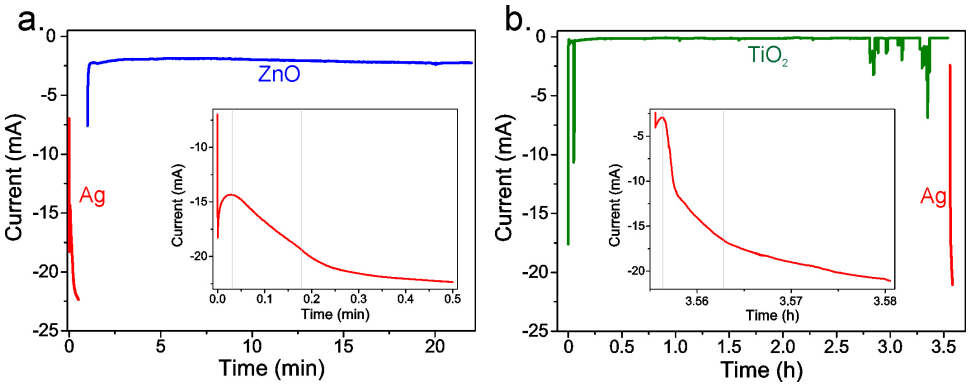

Figure 4. Typical I-t curves of (a) Ag|ZnO nanowire deposition, and (b) TiO_2-Ag nanowire deposition. The insets show an enlarged curve of the deposition of the Ag segment (**a**) or Ag core (**b**). Click here to view larger image.

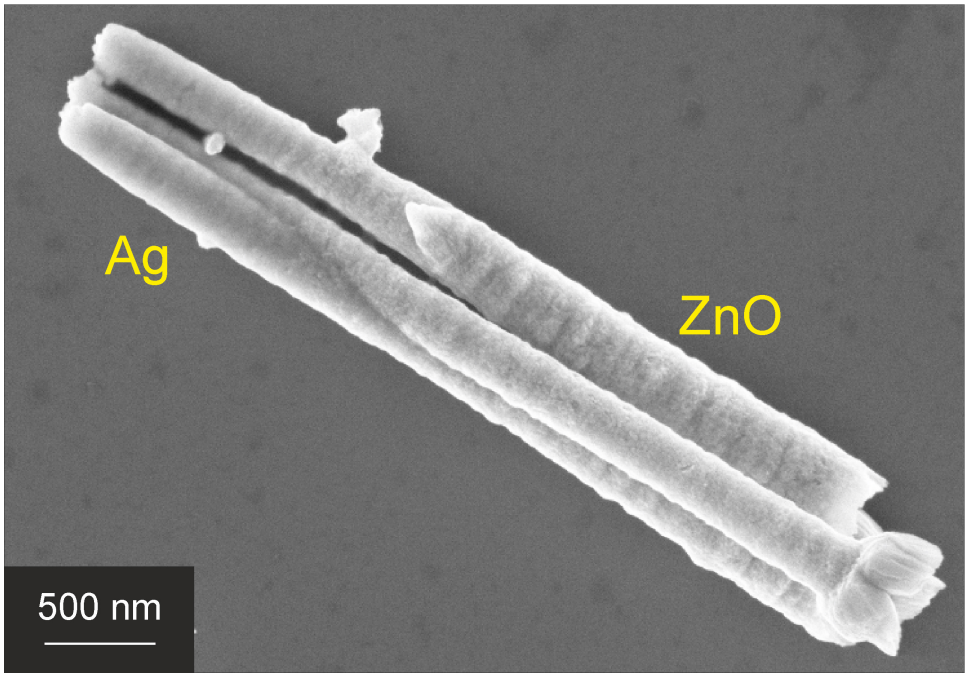

Figure 5. Scanning Electron Microscopy (SEM) picture of axially segmented ZnO|Ag nanowires.

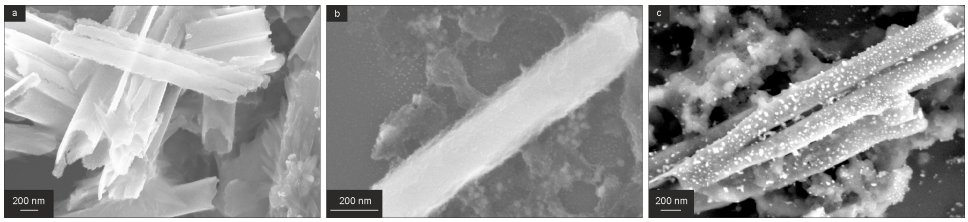

Figure 6. SEM pictures of (a) TiO_2 nanotubes, (b) coaxial TiO_2-Ag nanowire and (c) TiO_2/Ag nanotubes. Click here to view larger image.

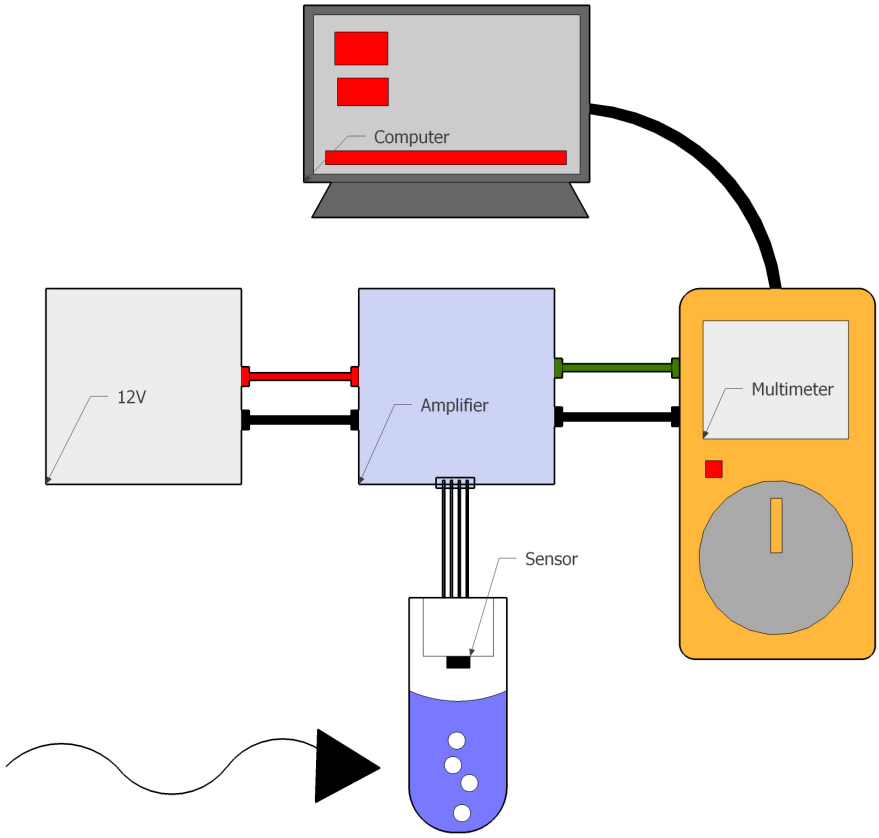

Figure 7. Typical setup for the detection of H_2 gas evolved from photocatalytic nanowires. The Pd based H_2 sensor is placed in the NS plug of a quartz cuvette, and connected to an amplifier (see **Figure 3**). The amplifier is operated by a 12 V power source and the signal from the sensor is read by a multimeter (or potentiostat) connected to a computer for graphical representation of the obtained signal. Click here to view larger image.

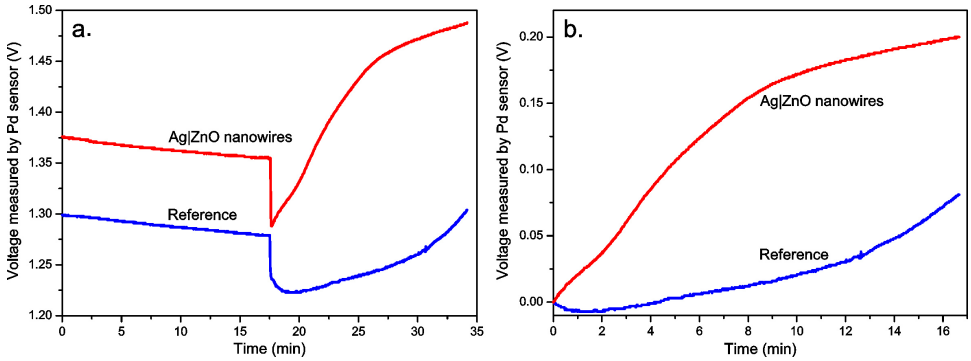

Figure 8. Response from the H_2 sensor during UV irradiation of Ag|ZnO nanowires in a methanol/water solution (red line) and reference experiment without nanowires (blue line). (**a**) Signal as measured by the sensor; (**b**) Signal during H_2 formation, where the data point at t = 17.5 min of (**a**) was defined as the start of the reaction in (**b**). Click here to view larger image.

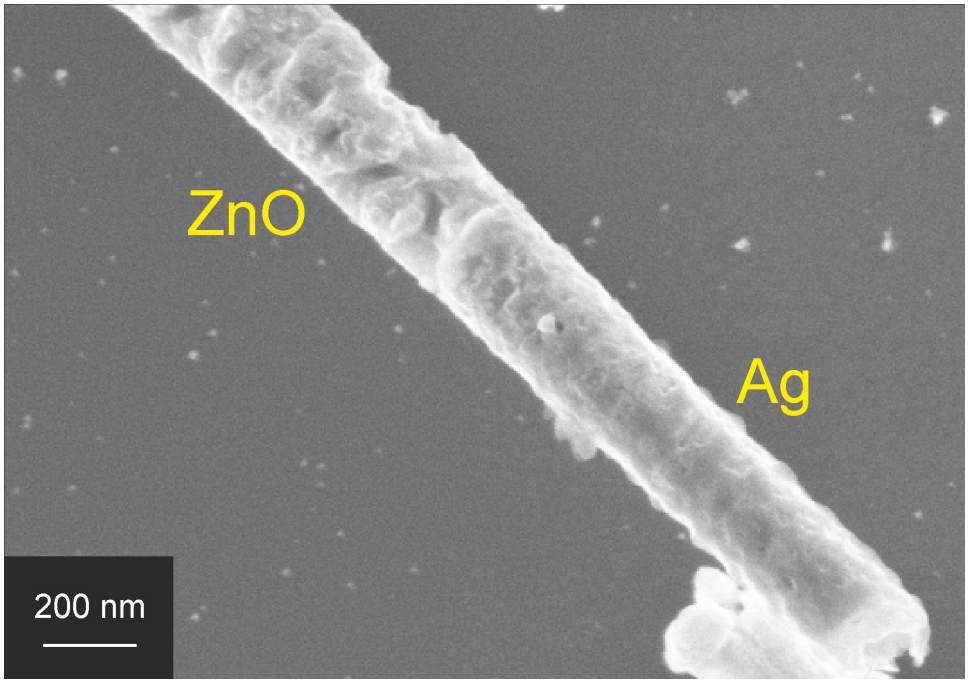

Figure 9. SEM image of photocorroded Ag|ZnO nanowire after 48 hr of UV illumination.

Discussion

Very important in the templated electrodeposition of nanowires is isolation of the back side of the gold electrode sputtered on top of the membrane. Without isolation, the material would preferentially deposit on the gold surface at the back side of the membrane instead of inside the pores. This is because the diffusion of ions to a flat electrode is much faster than diffusion into membrane pores. Another disadvantage of deposition on both sides of the gold electrode is that the obtained I-t curve cannot be related to the amount and length of deposited nanowires. In **Figure 4**, several stages can be identified for the deposition of the Ag segment (**a**) or Ag core (**b**). The first stage of every electrodeposition experiment is charging of the electrical double layer, which is accompanied by a sudden increase in current that slowly decreases as the electrical double layer reaches its equilibrium. As the PCTE membrane pores from Whatman have a cigar-shape, the current increases in the second stage as the surface area of deposition increases, leading to deposition of more material at the same time, and faster supply of reactants since the surface of the nanowire gets closer to the entrance of the membrane pores. In the third stage, the change in surface area is minimal, leading to a smaller slope of increasing current since only the effect of faster reactant supply is visible in this stage.

Please note that in the case of depositing segmented nanowires containing both a metal and an oxide segment, the order of electrodeposition inside the pores should be determined by taking the solubility of the deposited phases in each other's solution explicitly into account. In this case, the Ag segment was deposited before the ZnO segment as ZnO would dissolve in the acidic $AgNO_3$ solution. In the case of forming a segmented nanowire containing a noble metal and a less noble one, *e.g.* Pt and Ni, the galvanic replacement reaction of Ni by Pt should be taken into account. This galvanic replacement reaction can be suppressed by using a larger overpotential as discussed in a previous publication[54].

The choice for using either PCTE or AAO membranes for nanowire or nanotube synthesis is usually based on whether or not a thermal annealing step is desired for the material of choice. Without the necessity of an annealing step, PCTE membranes are easier to handle and relatively good membranes can be obtained commercially. For high temperature annealing, the use of AAO membranes is required. These membranes are not as flexible as the polycarbonate membranes and are very brittle. Some commercial AAO membranes are available, but the quality of homemade AAO membranes using a 2-step anodization is much better. For this, several recipes are available[55,56].

The Pd-based H_2 sensor used in this study is an easy and relatively cheap method for determining whether H_2 has formed or not. Unfortunately, it is not suitable for quantitative measurements due to its cross-sensitivity to volatile solvents like methanol, the intrinsic inability to detect dissolved H_2 in the methanol/water solution, and its non-linear response as seen in the shape of the curves in **Figure 8**. Quantitative measurements could be performed in a setup with a GC inlet connected to the head space above the methanol/water mixture, which is specialized equipment that is not available in every lab.

H_2 formation using Ag|ZnO nanowires typically ceased after ~48 hr of UV illumination as evidenced by terminated gas bubble formation. The reason for this loss of activity is photocorrosion of ZnO according to the following reaction[57-60]:

$$ZnO + 2h^+ \rightarrow Zn^{2+} + 1/2\ O_2 \quad (\mathbf{8})$$

An SEM image of photocorroded Ag|ZnO nanowires is shown in **Figure 9**. As can be seen from this figure, the surface of the ZnO segment became much rougher upon UV illumination as compared to the as-synthesized wires of **Figure 5**. When suspending another batch of Ag|ZnO nanowires in the same solution in the dark for 48 hr, no sign of corrosion was found. This confirmed that the observed corrosion indeed resulted from photocorrosion and not from electrolytic corrosion. In the literature, several methods have been reported for inhibition of ZnO

photocorrosion, including hybridization of ZnO nanoparticles with a monolayer of polyaniline or C_{60} and grafting of ZnO nanorods on TiO_2 nanotubes[59,61,62].

Templated electrodeposition of axially or radially segmented nanowires is a perfect platform for the deposition of multisegmented nanowires that are able to carry out more than one function at once, in which Ag|ZnO segments can be applied as photocatalytic elements. In a previous publication, an SEM image of a single nanowire containing six segments was introduced: Pt|Au|Pt|Ni|Ag|ZnO. Such a nanowire could be used for autonomous movement (Pt|Au|Pt), magnetic steering (Ni) and photocatalytic H_2 formation (Ag|ZnO)[53].

In summary, a simple protocol for the synthesis of segmented Ag|ZnO nanowires and coaxial TiO_2-Ag nanowires by templated electrodeposition is provided. A semi-quantitative method to determine the photocatalytic activity of such nanowires was demonstrated using the photocatalytic conversion of methanol and water into H_2 and CO_2 under UV illumination. It is envisaged that these metal oxide-metal nanowires can be used in multifunctional nanowires and other nanowire devices.

Disclosures

The authors declare that they have no competing financial interests.

The author, Eddy J.B. Rodijk is currently an employee of Twente Solid State Technology B.V., The Netherlands.

The author, Michiel G. Maas is currently an employee of Henkel AG & Co. KGaA, Germany.

Acknowledgements

Financial support from the Chemical Sciences division of the Netherlands Organization for Scientific Research (NWO-CW) in the framework of the TOP program is acknowledged.

References

1. Kuppler, R. J., *et al.* Potential applications of metal-organic frameworks. *Coordination Chemistry Reviews*. **253**, 3042-3066 (2009).
2. Hsu, C. L., *et al.* Well-aligned, vertically Al-doped ZnO nanowires synthesized on ZnO:Ga/glass templates. *Journal of The Electrochemical Society*. **152**, G378-G381 (2005).
3. Maas, M. G., Rodijk, E. J. B., Maijenburg, W., ten Elshof, J. E., & Blank, D. H. A. Photocatalytic segmented nanowires and single-step iron oxide nanotube synthesis: Templated electrodeposition as all-round tool. *MRS Proceedings*. Boston, MA, 1-6 (2010).
4. Mallouk, T. E., & Sen, A. Powering nanorobots: Catalytic engines enable tiny swimmers to harness fuel from their environment and overcome the weird physics of the microscopic world. *Scientific American*. **300**, 72-77 (2009).
5. Matei, E., Ion, L., Antohe, S., Neumann, R., & Enculescu, I. Multisegment CdTe nanowire homojunction photodiode. *Nanotechnology*. **21**, 105202 (2010).
6. Matei, E., *et al.* Sequential Deposition Of Multisegment Nanowires. *Digest Journal of Nanomaterials and Biostructures*. **5**, 1067-1076 (2010).
7. Maas, M. G., Rodijk, E. J. B., Maijenburg, A. W., Blank, D. H. A., & ten Elshof, J. E. Microstructure development in zinc oxide nanowires and iron oxohydroxide nanotubes by cathodic electrodeposition in nanopores. *Journal of Materials Research*. **26**, 2261-2267, doi:doi:10.1557/jmr.2011.93 (2011).
8. Jiang, H. L., Singh, S. K., Yan, J. M., Zhang, X. B., & Xu, Q. Liquid-Phase chemical hydrogen storage: Catalytic hydrogen generation under ambient conditions. *ChemSusChem*. **3**, 541-549 (2010).
9. Kubas, G. J. Hydrogen activation on organometallic complexes and H2 production, utilization, and storage for future energy. *Journal of Organometallic Chemistry*. **694**, 2648-2653 (2009).
10. Penner, R. M., & Martin, C. R. Preparation and electrochemical characterization of ultramicroelectrode ensembles. *Analytical*. **59**, 2625-2630 (1987).
11. Hurst, S. J., Payne, E. K., Qin, L., & Mirkin, C. A. Multisegmented one-dimensional nanorods prepared by hard-template synthetic methods. *Angewandte Chemie - International Edition*. **45**, 2672-2692, doi:10.1002/anie.200504025 (2006).
12. Cui, J. B., & Gibson, U. J. Electrodeposition and room temperature ferromagnetic anisotropy of Co and Ni-doped ZnO nanowire arrays. *Applied Physics Letters*. **87**, 1-3, doi:10.1063/1.2058222 (2005).
13. Lai, M., & Riley, D. J. Templated electrosynthesis of zinc oxide nanorods. *Chemistry of Materials*. **18**, 2233-2237, doi:10.1021/cm051613j (2006).
14. Zheng, M. J., Zhang, L. D., Li, G. H., & Shen, W. Z. Fabrication and optical properties of large-scale uniform zinc oxide nanowire arrays by one-step electrochemical deposition technique. *Chemical Physics Letters*. **363**, 123-128, doi:10.1016/s0009-2614(02)01106-5 (2002).
15. Sima, M., Enculescu, L., Enache, M., Vasile, E., & Ansermet, J. P. ZnO:Mn:Cu nanowires prepared by template method. *Physica Status Solidi (B) Basic Research*. **244**, 1522-1527, doi:10.1002/pssb.200675126 (2007).
16. Leprince-Wang, Y., Wang, G. Y., Zhang, X. Z., & Yu, D. P. Study on the microstructure and growth mechanism of electrochemical deposited ZnO nanowires. *Journal of Crystal Growth*. **287**, 89-93, doi:10.1016/j.jcrysgro.2005.10.049 (2006).
17. Leprince-Wang, Y., Yacoubi-Ouslim, A., & Wang, G. Y. Structure study of electrodeposited ZnO nanowires. *Microelectronics Journal*. **36**, 625-628, doi:10.1016/j.mejo.2005.04.033 (2005).
18. Ramirez, D., Pauporte, T., Gomez, H., & Lincot, D. Electrochemical growth of ZnO nanowires inside nanoporous alumina templates. A comparison with metallic Zn nanowires growth. *Physica Status Solidi (A) Applications and Materials Science*. **205**, 2371-2375, doi:10.1002/pssa.200779444 (2008).
19. Karuppuchamy, S., Nonomura, K., Yoshida, T., Sugiura, T., & Minoura, H. Cathodic electrodeposition of oxide semiconductor thin films and their application to dye-sensitized solar cells. *Solid State Ionics*. **151**, 19-27 (2002).
20. Miao, Z., *et al.* Electrochemically Induced Sol-Gel Preparation of Single-Crystalline TiO_2 Nanowires. *Nano Letters*. **2**, 717-720 (2002).

21. Otani, S., Katayama, J., Umemoto, H., & Matsuoka, M. Effect of bath temperature on the electrodeposition mechanism of zinc oxide film from zinc nitrate solution. *Journal of the Electrochemical Society*. **153**, C551-C556, doi:10.1149/1.2205187 (2006).
22. Yoshida, T., Komatsu, D., Shimokawa, N., & Minoura, H. Mechanism of cathodic electrodeposition of zinc oxide thin films from aqueous zinc nitrate baths. *Thin Solid Films*. **451-452**, 166-169, doi:10.1016/j.tsf.2003.10.097 (2004).
23. Natarajan, C., & Nogami, G. Cathodic electrodeposition of nanocrystalline titanium dioxide thin films. *Journal of the Electrochemical Society*. **143**, 1547-1550 (1996).
24. Karuppuchamy, S., *et al.* Cathodic electrodeposition of TiO_2 thin films for dye-sensitized photoelectrochemical applications. *Chemistry Letters*, 78-79 (2001).
25. Maijenburg, A. W., *et al.* Electrochemical synthesis of coaxial TiO_2-Ag nanowires and their application for photocatalytic water splitting. *Journal of Materials Chemistry A*. **2**, 2648-2656 (2014).
26. Wu, X. J., *et al.* Electrochemical synthesis and applications of oriented and hierarchically quasi-1D semiconducting nanostructures. *Coordination Chemistry Reviews*. **254**, 1135-1150 (2010).
27. Fujishima, A., & Honda, K. Electrochemical photolysis of water at a semiconductor electrode. *Nature*. **238**, 37-38 (1972).
28. Fujishima, A., Kohayakawa, K., & Honda, K. Hydrogen Production under Sunlight with an Electrochemical Photocell. *Journal of The Electrochemical Society*. **122**, 1487-1489 (1975).
29. Kudo, A., & Miseki, Y. Heterogeneous photocatalyst materials for water splitting. *Chemical Society Reviews*. **38**, 253-278 (2009).
30. Navarro Yerga, R. M., Consuelo Álvarez Galván, M., del Valle, F., Villoria de la Mano, J. A., & Fierro, J. L. Water splitting on semiconductor catalysts under visiblelight irradiation. *ChemSusChem*. **2**, 471-485 (2009).
31. Osterloh, F. E. Inorganic materials as catalysts for photochemical splitting of water. *Chemistry of Materials*. **20**, 35-54 (2008).
32. Khan, S. U. M., Al-Shahry, M., & Ingler Jr, W. B. Efficient photochemical water splitting by a chemically modified n-TiO_2. *Science*. **297**, 2243-2245 (2002).
33. Lin, W. C., Yang, W. D., Huang, I. L., Wu, T. S., & Chung, Z. J. Hydrogen production from methanol/water photocatalytic decomposition using Pt/TiO_2-xnx catalyst. *Energy and Fuels*. **23**, 2192-2196 (2009).
34. Ni, M., Leung, M. K. H., Leung, D. Y. C., & Sumathy, K. A review and recent developments in photocatalytic water-splitting using TiO_2 for hydrogen production. *Renewable and Sustainable Energy Reviews*. **11**, 401-425 (2007).
35. Rajeshwar, K. Hydrogen generation at irradiated oxide semiconductor-solution interfaces. *Journal of Applied Electrochemistry*. **37**, 765-787 (2007).
36. Service, R. F. Chemistry: Catalyst boosts hopes for hydrogen bonanza. *Science*. **297**, 2189-2190 (2002).
37. Gupta, M., *et al.* Preparation and characterization of nanostructured ZnO thin films for photoelectrochemical splitting of water. *Bulletin of Materials Science*. **32**, 23-30, doi:10.1007/s12034-009-0004-1 (2009).
38. He, J. H. *et al.* Electrical and photoelectrical performances of nano-photodiode based on ZnO nanowires. *Chemical Physics Letters*. **435**, 119-122 (2007).
39. Maeda, K., & Domen, K. Solid solution of GaN and ZnO as a stable photocatalyst for overall water splitting under visible light. *Chemistry of Materials*. **22**, 612-623 (2010).
40. Yang, X., *et al*. Nitrogen-doped ZnO nanowire arrays for photoelectrochemical water splitting. *Nano Letters*. **9**, 2331-2336 (2009).
41. Ekambaram, S. Photoproduction of clean H_2 or O_2 from water using oxide semiconductors in presence of sacrificial reagent. *Journal of Alloys and Compounds*. **448**, 238-245 (2008).
42. Mohapatra, S. K., John, S. E., Banerjee, S., & Misra, M. Water photooxidation by smooth and ultrathin R-Fe2O3 nanotube arrays. *Chemistry of Materials*. **21**, 3048-3055 (2009).
43. Best, J. P., & Dunstan, D. E. Nanotechnology for photolytic hydrogen production: Colloidal anodic oxidation. *International Journal of Hydrogen Energy*. **34**, 7562-7578 (2009).
44. Hochbaum, A. I., & Yang, P. Semiconductor nanowires for energy conversion. *Chemical Reviews*. **110**, 527-546 (2010).
45. Kudo, A. Recent progress in the development of visible light-driven powdered photocatalysts for water splitting. *International Journal of Hydrogen Energy*. **32**, 2673-2678 (2007).
46. Li, J., & Zhang, J. Z. Optical properties and applications of hybrid semiconductor nanomaterials. *Coordination Chemistry Reviews*. **253**, 3015-3041 (2009).
47. Yi, H., Peng, T., Ke, D., Zan, L., & Yan, C. Photocatalytic H2 production from methanol aqueous solution over titania nanoparticles with mesostructures. *International Journal of Hydrogen Energy*. **33**, 672-678 (2008).
48. Zäch, M., Hägglund, C., Chakarov, D., & Kasemo, B. Nanoscience and nanotechnology for advanced energy systems. *Current Opinion in Solid State and Materials Science*. **10**, 132-143 (2006).
49. Zhu, J., & Zäch, M. Nanostructured materials for photocatalytic hydrogen production. *Current Opinion in Colloid and Interface Science*. **14**, 260-269 (2009).
50. Martin, C. R. Nanomaterials: A membrane-based synthetic approach. *Science*. **266**, 1961-1966 (1994).
51. Nozik, A. J. Photochemical diodes. *Applied Physics Letters*. **30**, 567-569 (1977).
52. Bahnemann, D. W., Kormann, C., & Hoffmann, M. R. Preparation and characterization of quantum size zinc oxide: A detailed spectroscopic study. *Journal of Physical Chemistry*. **91**, 3789-3798 (1987).
53. Maijenburg, A. W., *et al.* Hydrogen generation from photocatalytic silver|zinc oxide nanowires: Towards multifunctional multisegmented nanowire devices. *Small*. **7**, 2709-2713, doi:10.1002/smll.201101198 (2011).
54. Maijenburg, A. W., *et al.* Electrodeposition of micropatterned NiPt multilayers and segmented NiPtNi nanowires. *Electrochimica Acta*. **81**, 123-128, doi:10.1016/j.electacta.2012.07.095 (2012).
55. Masuda, H., Yada, K., & Osaka, A. Self-ordering of cell configuration of anodic porous alumina with large-size pores in phosphoric acid solution. *Japanese Journal of Applied Physics, Part 2: Letters*. **37**, L1340-L1342 (1998).
56. Nielsch, K., Müller, F., Li, A. P., & Gösele, U. Uniform nickel deposition into ordered alumina pores by pulsed electrodeposition. *Advanced Materials*. **12**, 582-586, doi:10.1002/(sici)1521-4095(200004)12:8<582::aid-adma582>3.0.co;2-3 (2000).
57. Chen, X., *et al.* Fabrication of sandwich-structured ZnO/reduced graphite oxide composite and its photocatalytic properties. *Journal of Materials Science*. **45**, 953-960 (2010).
58. Doménech, J., & Prieto, A. Stability of ZnO particles in aqueous suspensions under UV illumination. *Journal of Physical Chemistry*. **90**, 1123-1126 (1986).
59. Fu, H., Xu, T., Zhu, S., & Zhu, Y. Photocorrosion inhibition and enhancement of photocatalytic activity for ZnO via hybridization with C60. *Environmental Science and Technology*. **42**, 8064-8069 (2008).

60. Kislov, N., *et al.* Photocatalytic degradation of methyl orange over single crystalline ZnO: Orientation dependence of photoactivity and photostability of ZnO. *Langmuir*. **25**, 3310-3315 (2009).
61. Lei, Y., *et al.* Fabrication, characterization, and photoelectrocatalytic application of ZnO nanorods grafted on vertically aligned TiO2 nanotubes. *Journal of Physical Chemistry C*. **113**, 19067-19076 (2009).
62. Zhang, H., Zong, R., & Zhu, Y. Photocorrosion inhibition and photoactivity enhancement for zinc oxide via hybridization with monolayer polyaniline. *Journal of Physical Chemistry C*. **113**, 4605-4611 (2009).